Notes

Synthesis and Characterization of the Dodecahexaynediyldiiron Complex, Fp*−(C≡C)$_6$−Fp* [Fp*= Fe(η^5-C$_5$Me$_5$)(CO)$_2$], the Longest Structurally Characterized Polyynediyl Complex

Aizoh Sakurai, Munetaka Akita,* and Yoshihiko Moro-oka*

Research Laboratory of Resources Utilization, Tokyo Institute of Technology, 4259 Nagatsuta, Midori-ku, Yokohama 226-8503, Japan

Received April 14, 1999

Summary: Cu-catalyzed oxidative coupling of the hexatriynyl complex Fp−(C≡C)$_3$−H affords the dodecahexynediyl diiron complex Fp*−(C≡C)$_6$−Fp*. Its linear but slightly twisted structure has been revealed by X-ray crystallography.*

Polyynediyl complexes, M−(C≡C)$_n$−M, have been studied mainly from two different viewpoints. One is the synthetic study of polynuclear complexes with polycarbon ligands, and the other is the study of electron-transfer processes through the pπ-conjugated system of the carbon rod extended to the metal termini.[1] In the latter system, it is expected that the two metal termini can communicate through the conjugated system. The carbon chain length is extended to C_{20} as reported by Gladysz, but it is also reported that, as the carbon chain is elongated, communication between the two metal centers becomes less effective.[2]

We have been carrying out the synthetic study of polycarbon cluster compounds.[3] In previous papers, we reported (i) synthesis of polyynediyldiiron complexes Fp*−(C≡C)$_n$−Fp* (n = 1, 2, 3, 4) and polyynyliron complexes Fp*−(C≡C)$_n$−H (n = 1, 2)[3c] and (ii) their conversion to polynuclear complexes via addition of polymetallic fragments to the (C≡C)$_n$ moiety.[3d,e] Though this type of chemistry is related to the polynuclear acetylide cluster compounds,[4] we have often encountered new reactions, which have never been observed for the classical acetylide cluster compounds. For example, (1) the trinuclear acetylide cluster-type C_2 complexes (μ-C≡C−Fp*)M$_2$FeCp*(CO)$_n$ [n = 6 (M = Co), n = 7 (M = Fe)] display dynamic behavior by way of reversible metal−metal bond scission−recombination processes,[3d,5a] (2) sequential conversion of the ethynediyl complex Fp*−C≡C−Fp* (a permetalated ethyne) to permetalated ethene and ethane structures has been observed,[5b] and (3) C≡C bond cleavage giving a bis(μ_3-alkylidyne) complex has been observed for the hexatriynediyl and octatetraynediyl complexes.[3e] Herein we disclose synthesis and structure determination of the dodecahexaynediyldiiron complex **1**, Fp*−(C≡C)$_6$−Fp*, the longest polyynediyl complex of the Fp* system.[6]

Scheme 1

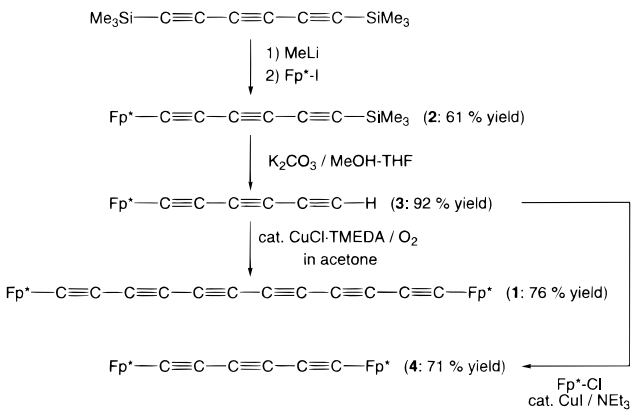

Results and Discussion

The synthetic route to the dodecahexaynediyl complex **1** summarized in Scheme 1 follows the conventional synthetic method for polyynediyl complexes, i.e., copper-catalyzed oxidative coupling of the ynyl complex.[1−3,7] The trimethylsilylhexatriynyl complex **2** was prepared by alkynylation of Fp*−I with trimethylsilylhexatri-

(1) (a) Bartik, T.; Weng, W.; Ramsden, J. A.; Szafert, S.; Falloon, S. B.; Arif, A. M.; Gladysz, J. A. *J. Am. Chem. Soc.* **1998**, *120*, 11071. (b) Guillemot, M.; Toupet, L.; Lapinte, C. *Organometallics* **1998**, *17*, 1928. (c) See references cited in refs 1a,b and 3c.

(2) (a) Bartik, T.; Bartik, B.; Brady, M.; Dembinski, R.; Gladysz, J. A. *Angew. Chem., Int. Ed. Engl.* **1996**, *35*, 414. (b) Brady, M.; Weng, W.; Zhou, Y.; Seylet, J. W.; Amoroso, A. J.; Arif, A. M.; Böhme, M.; Frenking, G.; Gladysz, J. A. *J. Am. Chem. Soc.* **1997**, *119*, 775.

(3) C_2 complex: (a) Akita, M.; Moro-oka, Y. *Bull. Chem. Soc. Jpn.* **1995**, *68*, 420. C_1 complex: (b) Takahashi, Y.; Akita, M.; Moro-oka, Y. *J. Chem. Soc., Chem. Commun.* **1997**, 1557. C_n complex (n ≥ 4): (c) Akita, M.; Chung, M.-C.; Sakurai, A.; Sugimoto, S.; Terada, M.; Tanaka, M.; Moro-oka, Y. *Organometallics*, **1997**, *16*, 4882. (d) Akita, M.; Chung, M.-C.; Terada, M.; Miyauti, M.; Tanaka, M.; Moro-oka, Y. *J. Organomet. Chem.*, **1998**, *565*, 49. (e) Akita, M.; Sakurai, A.; Moro-oka, Y. *J. Chem. Soc., Chem. Commun.* **1999**, 101.

(4) See, for example: (a) Sappa, E.; Tiripicchio, A.; Braunstein, P. *Chem. Rev.* **1983**, *83*, 203. (b) Raithby, P. R.; Rosales, M. J. *Adv. Inorg. Chem. Radiochem.* **1985**, *29*, 169.

(5) (a) Akita, M.; Terada, M.; Moro-oka, Y. *Organometallics* **1992**, *11*, 1825. (b) Akita, M.; Sugimoto, S.; Tanaka, M.; Moro-oka, Y. *J. Am. Chem. Soc.* **1992**, *114*, 7581. (c) Akita, M.; Terada, M.; Oyama, S.; Moro-oka, Y. *Organometallics* **1990**, *9*, 816.

(6) Abbreviations used in this paper: Cp*= η^5-C$_5$Me$_5$; Fp*= Cp*Fe(CO)$_2$.

10.1021/om990266i CCC: $18.00
Publication on Web 07/17/1999

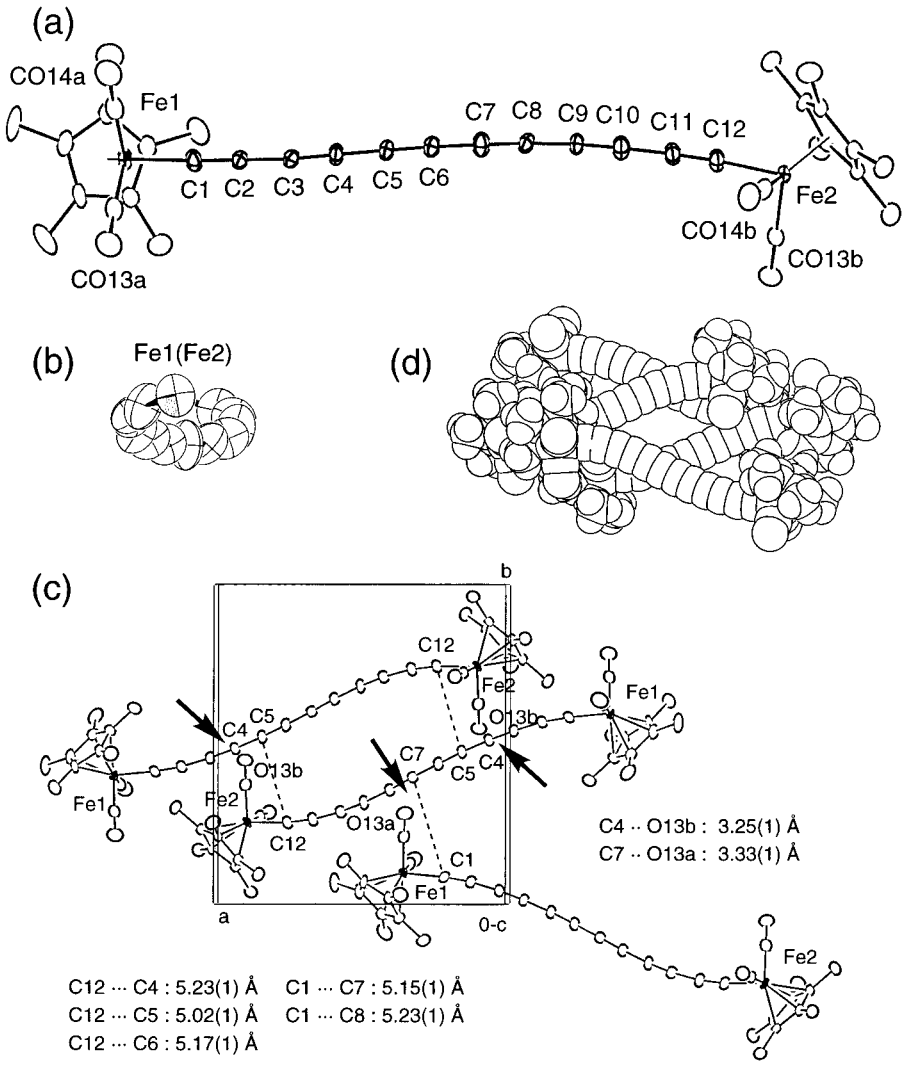

Figure 1. (a) An overview of **1**. (b) A down view of the (μ-C_{12})Fe_2 rod from the Fe1 side. (c) Intermolecular interactions. (d) Cavity among the C_{12} rods.

ynyllithium generated by treatment of bis(trimethylsilyl)hexatriyne with methyllithium. Subsequent desilylation with potassium carbonate in MeOH−THF gave the hexatriynyl complex **3**, which was converted to the desired complex **1** by oxidative dimerization in the presence of a catalytic amount of CuCl·TMEDA complex. Cu-catalyzed metalation of hexatriynyl complex **3** with Fp*−Cl afforded the hexatriynediyl complex **4**.

The hexatriynyl complex **3** and the dodecahexaynediyl complex **1** were readily characterized by the ^{13}C NMR spectra containing six alkynyl carbon signals. Their spectroscopic features will be discussed later as compared with those of the related compounds.

The molecular structure of the dodecahexaynediyl complex **1** has been determined by X-ray crystallography. Views of **1** are shown in Figure 1, and the structural parameters are compared with the shorter congeners (Chart 1), the ethynediyl [μ-C_2; **5** (η^5-C_5Me_4-Et derivative)][6] and butadiynediyl complexes (μ-C_4; **6**). The Fe−(C≡C)$_6$−Fe linkage, where the two Fe atoms separated by ca. 17.56 Å are spanned with the C_{12}-polyyne bridge, can be primarily viewed as a carbon rod. But the rod is considerably twisted as can be seen from Figure 1b, and the nonlinearity can be estimated by the sum and average of deviation of the bond angles from 180°, which are 2.8°/1.4° (**5**), 8.0°/2.0° (**6**), and 57.5°/4.8° (**1**), respectively. As for the polyyne part, clear short−long C≡C−C bond alternation is observed. The averaged values for the C≡C and ≡C−C≡ bond lengths are 1.21

Chart 1. Selected Structural Parameters for the Polyynediyldiiron Complexes (Bond Lengths in Å and Bond Angles in deg)

1.23(1) 1.20(1) 1.22(1) 1.23(1) 1.19(1) 1.20(1)
Fe1—C1≡C2—C3≡C4—C5≡C6—C7≡C8—C9≡C10-C11≡C12—Fe2 (**1**)
1.878(9) 1.36(1) 1.35(1) 1.35(1) 1.36(1) 1.38(1) 1.888(8)

175.2(6) 175.5(8) 176.3(9) 178(1) 175.1(9) 171.7(9)
Fe1—C1≡C2—C3≡C4—C5≡C6—C7≡C8—C9≡C10-C11≡C12—Fe2 (**1**)
172.7(8) 176.8(9) 177(1) 176.9(9) 173.8(9) 173.3(7)

1.929(3) 1.206(6) 1.929(3) 1.933(4) 1.197(4) 1.396(7) 1.197(4) 1.933(4)
Fp#—C≡C—Fp# (**5**) Fp*—C≡C—C≡C—Fp* (**6**)
178.6(6) 178.6(6) 178.0(4) 178.0(6) 178.0(6) 178.0(4)

(7) (a) Coat, F.; Lapinte, C. *Organometallics* **1996**, *15*, 477. (b) Bruce, M. I.; Ke, M.; Low, P. J. *J. Chem. Soc., Chem. Commun.* **1996**, 2405. (c) Reference 2. (d) Taylor, R. J. *Practical Approach Series in Organic Synthesis: Organocopper Reagents*; Oxford University Press: Oxford, U.K., 1995.

Scheme 2

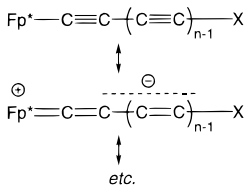

and 1.36 Å, respectively. Although the C≡C lengths are comparable to those in **5** and **6**, the C−C distances are slightly shorter than those in **6** (by 0.03 Å). In contrast to the similarity in the $(C{\equiv}C)_n$ parts, the Fe−C lengths of **1** (averaged value: 1.88 Å) are substantially shorter than those in **5** and **6** (ca. 1.93 Å). These structural distortions can be interpreted in terms of the extent of contribution of vinylidene-type resonance structure (Scheme 2). The anionic charge can be widely delocalized over the longer carbon chain, and as a result, the contribution of the zwitterionic structure becomes more evident for **1**; i.e., the Fe−C and C−C distances of **1** are shorter than those of **5** and **6**. As for the C≡C distances, it is known that they are less sensitive to the electronic state of the C≡C bond. For example, no significant difference is found for the C≡C lengths in acetylene (1.20 Å) and the polyynediyl complexes.

Let us discuss intermolecular interactions, which are shown in Figure 1c. Close contacts shorter than 2.8 Å are found among the hydrogen atoms of the Cp* ligands and between the Cp* hydrogen atom and the CO ligands. The closest interactions among non-hydrogen atoms (indicated by arrows in Figure 1c) are found between the C_{12} rod and the CO ligands [C4···O13b, 3.25 Å; C7···O13a, 3.33(1) Å]. On the other hand, separations between the C_{12} rods (indicated by dotted lines in Figure 1c) are longer than 5 Å, and as a result, a cavity is formed as can be seen from Figure 1d. Thus no significant interaction among the C_{12} rods is found, although weak interactions (>2.8 Å) with the Cp* hydrogen atoms are found. The C≡C parts in polyynediyl complexes are usually basic enough to make a hydrogen-bonding interaction with an acidic substrate, and cavities are often filled up by such a substrate or solvent to result in better crystal packing. For example, the C≡C moiety in the Cp* derivative of **5** is hydrogen-bonded with methanol,[3c] and it was reported that the highly basic gold ethynediyl complex $(\mu\text{-}C_2)[Au(PR_3)_3]_2$ formed a hydrogen-bonding interaction with $CHCl_3$.[8] Thus it may be concluded that the crystal packing of **1** is controlled dominantly by the intermolecular interactions of the Fp* moieties rather than those of the C_{12} carbon rods. According to the CSD database, the dodecahexaynediyl complex **1** is the longest polyyne compound characterized by X-ray crystallography.

^{13}C NMR and IR data for **1**, **3,** and **4** are summarized in Table 1 and compared with related compounds. The spectroscopic features can also be interpreted in terms of Scheme 2. Most of the ^{13}C NMR signals of the polyynyl complexes $Fp^*{-}(C{\equiv}C)_n{-}H$ can be assigned on the basis of the magnitude of the J_{C-H} values. The three singlets of **3** are tentatively assigned by comparison with the data for the other ynyl complexes. In contrast, the assignment of the polyynediyl complexes are not straightforward, because they contain only singlet $(C{\equiv}C)_n$ signals. The most deshielded signals, however, may be assigned to the α-carbon atoms by comparison with the ynyl complexes, and this assignment should be reasonable, when contribution of the vinylidene structure is taken into account. It is well-established that the α-carbon signals of vinylidene complexes are highly deshielded and usually appear below 300 ppm.[9] The downfield shift of the C_α signals may be a result of contribution of the vinylidene structure. It is notable that as the carbon rods $(C{\equiv}C)_n$ and $(C{\equiv}C)_n{-}H$ become longer, the C_α signal is shifted to lower field, and a shift of the CO stretching vibration of the Fp* groups to higher energies is also observed. These tendencies can be explained by the increased contribution of the zwitterionic vinylidene structure for a complex with the longer carbon chain. The zwitterionic form with the negative charge developed on the carbon rod may be more effectively stabilized by delocalization over a longer carbon chain. This means that as the carbon rod becomes longer, the contribution of the vinylidene structure becomes evident. As a result, the α-carbon signal is shifted to lower field and the C≡O vibration is shifted to higher energies due to the decreased electron density at the metal center.

The reactivity of the polyynediyl complexes is now under study and a portion of the results was already reported.[3e]

Experimental Section

General Methods. All manipulations were carried out under an inert atmosphere by using standard Schlenk techniques. Ether, THF, and hexane (Na−K alloy), MeOH ($Mg(OMe)_2$), and CH_2Cl_2 (CaH_2) were treated with appropriate drying agents, distilled, and stored under argon. ^{1}H and ^{13}C NMR spectra were recorded on a JEOL EX400 (^{1}H, 400 MHz; ^{13}C, 100 MHz) spectrometer. Solvents for NMR measurements containing 0.5% TMS were dried over molecular sieves, degassed, distilled under reduced pressure, and stored under Ar. IR and FD−MS spectra were obtained on a JASCO FT/IR 5300 spectrometer and a Hitachi M80 mass spectrometer, respectively. $Me_3Si{-}(C{\equiv}C)_3{-}SiMe_3$,[10] $Fp^*{-}Cl$,[11] and $Fp^*{-}I$ [11] were prepared according to the reported methods.

Synthesis of $Fp^*{-}(C{\equiv}C)_3{-}SiMe_3$ (2). To a THF solution (8 mL) of $Me_3Si{-}(C{\equiv}C)_3{-}SiMe_3$ (894 mg, 4.09 mmol) was added an ethereal solution of MeLi (1.15 M, 3.1 mL, 3.5 mmol), and the mixture was stirred for 3.5 h. The resultant mixture was cooled to −78 °C in a dry ice−methanol bath, and a THF solution (10 mL) of $Fp^*{-}I$ (937 mg, 2.51 mmol) was added dropwise. After 10 min, the cooling bath was removed and the mixture was stirred for 3 h at ambient temperature. After formation of **2** was checked by TLC, MeOH (1 mL) was added to destroy excess lithium reagents, and the volatiles were removed under reduced pressure. Products were extracted with ether, and inorganic salts were removed by filtration through an alumina pad. Product **2** was obtained as yellow solids by precipitation by addition of hexane. A small amount of **2** was recovered by concentration of the supernatant solution (600 mg. 1.53 mmol, 61% yield). ^{1}H NMR ($CDCl_3$): δ 1.84 (15H, s, Cp*), 0.15 (9H, s, $SiMe_3$).

(8) Müller, T. E.; Choi, S. W.-K.; Mingos, D. M. P.; Murphy, D.; Williams, D. J.; Yam, V. W.-W. *J. Organomet. Chem.* **1994**, *179*, 394.

(9) Bruce, M. I. *Chem. Rev.* **1998**, *98*, 2797. See also references cited therein.

(10) Rubin, Y.; Lin, S. S.; Knobler, C. B.; Anthony, J.; Boldi, A. M.; Diedrich, F. *J. Am. Chem. Soc.* **1991**, *113*, 6943.

(11) Akita, M.; Terada, M.; Tanaka, M.; Moro-oka, Y. *J. Organomet. Chem.* **1996**, *510*, 255.

Table 1. Comparison of ^{13}C NMR and IR Data for the Polyynyl and Polyynediyl Iron Complexes[a]

n	C_α	C_β	C_γ	C_δ	C_ϵ	C_ζ	ν(C≡C)	ν(C≡O)
Polyynyl Complexes Fp*−(C≡C)$_n$−H								
1[b]	97.0 (55)	97.5 (227)					*c*	2022, 1967
2[d]	106.4	92.8 (7)	71.9 (50)	53.5 (252)			2041	2027, 1977
3 (**3**)	114.6[e]	93.7[e]	64.5[e]	48.6 (7)	70.4 (52)	61.7 (255)	2158, 2100	2030, 1982
Polyynediyl Complexes Fp*−(C≡C)$_n$N−Fp*								
1[b]	98.1						*c*	1996, 1951
2[d]	101.6[e]	66.8[e]					2150	2020, 1967
3 (**4**)	99.7[e]		54.0, 94.9 [f]				2094	2020, 1974
4[d]	110.8[e]		51.4, 61.6, 94.8 [f]				2136, 2088	2028, 1981
6 (**1**)	118.3[e]		50.5, 58.9, 62.2, 64.8, 94.6 [f]				2123, 2087	2028, 1981

[a] ^{13}C NMR chemical shifts in ppm and IR data (CH_2Cl_2 solutions) in cm^{-1}. C−H coupling constants (in Hz) for the doublet signals are shown in parentheses. Fe−C_α−C_β−C_γ−C_δ−C_ϵ−C_ζ. [b] Reference 5c. [c] Not observed. [d] Reference 3c. [e] Tentatively assigned. [f] Not assigned.

Synthesis of Fp*−(C≡C)$_3$−H (3). K_2CO_3 (215 mg, 1.56 mmol) was added to **2** (611 mg, 1.56 mmol) dissolved in a mixture of THF (10 mL) and MeOH (10 mL), and the resultant mixture was stirred for 2 h at ambient temperature. After the consumption of **2** was checked by TLC, the volatiles were removed by TLC. Extraction with CH_2Cl_2 followed by filtration through an alumina pad and precipitation by addition of hexane gave **3** as yellow brown solids (482 mg, 1.43 mmol, 92%). ^1H NMR ($CDCl_3$): δ_H 1.85 (15H, s, Cp*), 1.75 (1H, s, C_6H). Anal. Calcd for $C_{18}H_{16}O_2Fe$: C, 67.53; H, 5.04. Found: 67.00; H, 5.21.

Synthesis of Fp*−(C≡C)$_6$−Fp* (1). TMEDA (0.2 mL, 1.72 mmol) was added to an acetone suspension (12 mL) of CuCl (100 mg, 1.01 mmol) and the mixture was stirred vigorously for 30 min. The blue green supernatant was used as a stock solution of CuCl·TMEDA catalyst. Into a four-necked flask equipped with gas inlet, gas outlet, a thermometer, and a rubber septum, **3** (602 mg, 1.88 mmol) was weighed and acetone (50 mL) was added. Then from the gas inlet O_2 gas was passed through the solution. Each 1 mL portion of the CuCl·TMEDA catalyst was added via a syringe through the rubber septum for ca. 30 min. The addition rate was adjusted so that the temperature should be kept below 30 °C. After addition of the Cu catalyst, the mixture was further stirred for 3 h with O_2 bubbling. The product appeared as yellow precipitates during the reaction. After consumption of **3** was confirmed by TLC, the volatiles were removed under reduced pressure. The product was extracted with CH_2Cl_2 and passed through an alumina pad. The filtrate was concentrated under reduced pressure and the resulting yellow precipitates were washed with CH_2Cl_2−ether−hexane mixed solvent twice and dried under reduced pressure to give **1** (yellow brown solids, 455 mg, 7.13 mmol, 76% yield). Anal. Calcd for $C_{37}H_{32}O_4Fe_2Cl_2$ (**4**·CH_2Cl_2): C, 61.45; H, 4.46. Found: 61.83; H, 4.21.

Synthesis of Fp*−(C≡C)$_3$−Fp* (4). CuI (28 mg, 0.15 mmol) was added to NEt_3 (3 mL; degassed twice). After the mixture was stirred for 10 min, a THF solution (15 mL) of **3** (482 mg, 1.50 mmol) was added to the CuI solution, and the mixture was further stirred for 30 min. Then a THF solution (5 mL) of Fp*−Cl (425 mg, 1.50 mmol) was added to the mixture, and stirring was continued for 7 h. The product appeared as orange precipitates. Evaporation of the volatiles, extraction with CH_2Cl_2, filtration through an alumina pad, and evaporation of the volatiles left an orange residue, which was washed with cold ether (−78 °C) twice to yield **4** (orange powders, 607 mg, 1.07 mmol, 71% yield). Despite several attempts, an analytically pure sample could not be obtained.

X-ray Crystallography. Single crystals of **1** were obtained by recrystallization from CH_2Cl_2−hexane and mounted on a glass fiber.

Table 2. Crystallographic Data for 1

formula	$C_{36}H_{30}O_4Fe_2$	*Z*	4
fw	638.3	d_{calcd}/g·cm^{-3}	1.36
cryst syst	monoclinic	μ/cm^{-1}	9.7
space group	$P2_1/c$	2θ/deg	up to 55
a/Å	12.997(5)	no of params refined	389
b/Å	14.390(3)	R1 for data with	0.086
c/Å	16.705(8)	$F_o > 4\sigma(F_o)$	(3409 data)
β/deg	91.064(2)	wR2	0.197
V/Å^3	3124(2)	for all data	(4588 data)

Diffraction measurements were made on a Rigaku RAXIS IV imaging plate area detector with Mo Kα radiation (λ = 0.710 69 Å). The data collections were carried out at −60 °C. Indexing was performed from three oscillation images which were exposed for 4 min. The crystal-to-detector distance was 110 mm. Data collection parameters were as follows: oscillation range, 6.0°; number of oscillation images, 22; exposed time, 180 min. Readout was performed with a pixel size of 100 μm × 100 μm.

The structural analysis was performed on an IRIS O2 computer using the teXsan structure solving program system obtained from the Rigaku Corp., Tokyo, Japan. Neutral scattering factors were obtained from the standard source.[12] In the reduction of data, Lorentz and polarization corrections were made. An empirical absorption correction was also made.[13] Crystallographic data are summarized in Table 2.

The structure was solved by a combination of the direct methods (SHELXL 87 and DIRDIF). Non-hydrogen atoms were refined with anisotropic thermal parameters, and the methyl hydrogen atoms were refined using riding models.

Acknowledgment. We are grateful to the Ministry of Education, Science, Sports, and Culture of the Japanese Government for financial support of this research.

Supporting Information Available: Crystallographic information including tables of postional parameters and B_{eq}, anisotropic thermal parameters, and interatomic distances and bond angles and a figure showing the atomic numbering scheme for **1**. This material is available free of charge via the Internet at http://pubs.acs.org.

OM990266I

(12) *International Tables for X-ray Crystallography*; Kynoch Press: Birmingham, U.K., 1975; Vol. 4.
(13) Stuart, D.; Walker, N. *Acta Crystallogr.* **1979**, *A35*, 925.